Nanoscale

Accepted Manuscript

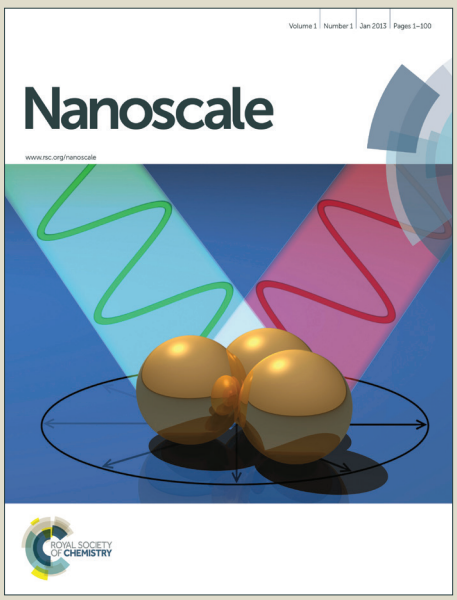

ROYAL SOCIETY OF CHEMISTRY

www.rsc.org/nanoscale

Sulphur doping: a facile approach to tune the electronic structure and optical properties of graphene quantum dots

Xueming Li, [a] Shu Ping Lau,*[b] Libin Tang, [b,c] Rongbin Ji, [c] and Peizhi Yang*[a]

Received (in XXX, XXX) Xth XXXXXXXXX 20XX, Accepted Xth XXXXXXXXX 20XX
DOI: 10.1039/b000000x

Sulphur-doped carbon-based materials have attracted a great deal of interest because of the important applications in the fields of oxygen reduction reactions, hydrogen storages, supercapacitors, photocatalysts and lithium ion batteries. Here, we report a new member of sulphur-doped carbon-based materials, *i.e.* sulphur doped graphene quantum dots (S-GQDs). The S-GQDs were prepared by a hydrothermal method using fructose and sulphuric acid as source materials. Absorption and photoluminescence investigations show that inter-band crossings are responsible for the observed multiple emission peaks. The incorporation of ~1 at.% of S into the quantum dots can effectively modify the electronic structure of the S-GQDs by introducing S-related energy levels between π and π^* of C. The additional energy levels in the S-GQDs lead to efficient and multiple emission peaks.

Introduction

Recently, sulphur-doped carbon-based materials have aroused great interests due to their unique properties induced by sulphur doping. These properties includes, electrocatalytic activity,[1] hydrogen adsorption,[2] high electrochemical capacity,[3] rechargeable battery performance,[4] photoactivity,[5] and p-type semiconductor property [6]. Consequently, sulphur-doped carbon-based materials have been utilised in oxygen reduction reactions,[1,7-10] hydrogen storage,[2,11] supercapacitor,[3] photocatalyst,[5,12] lithium-oxygen battery,[4] lithium ion battery,[13] and field effect transistor.[6] Up to now, various sulphur-doped carbon-based materials were reported such as microporous carbon,[2] carbon microsphere,[11] activated carbon,[5] graphene,[1,6-8] and co-doped graphene.[9]

The doping of sulphur in carbon framework makes sulphur doped carbon-based materials attractive; however, the understanding of the optical properties induced by sulphur doping remains an open question. It is not clear that whether the effectiveness of sulphur doping can be retained as the size of the carbon-based materials reduces to nanoscale? If yes, what are the configurations of sulphur in graphene quantum dot (S-GQD)? Can the incorporation of sulphur modify the energy level of GQD?

The sulphur and nitrogen co-doped carbon dots[14] and GQDs[15] were demonstrated and showed attractive applications. The preparation of the sulphur-doped GQDs have not been achieved. Therefore, it is desirable to develop an approach to prepare S-GQDs with high crystal quality. It is of scientific interest and technical importance to study the structure and optical properties of S-GQDs.

Here we report a facile method to prepare sulphur-doped GQDs by using fructose and sulphuric acid as source materials. The method is environmentally friendly, effective and scalable. The structure of the S-GQDs and the configurations of sulphur in S-GQDs have been investigated. The tuning of electronic structure and optical properties of the GQDs by sulphur doping is realized.

Experimental

S-GQDs preparation

S-GQDs were prepared using a hydrothermal method with temperature at 170 ℃ for 4 hours. The source materials are fructose and sulphuric acid. The S-GQDs samples were dialyzed by molecular weight cut-off (MWCO) of 1000 against DI water for purification.

S-GQDs characterizations

All the characterizations were performed at room temperature. Transmission electron microscopy of the samples was performed on a JEOL (JEM-2100F) at operating voltage of 200 kV. The

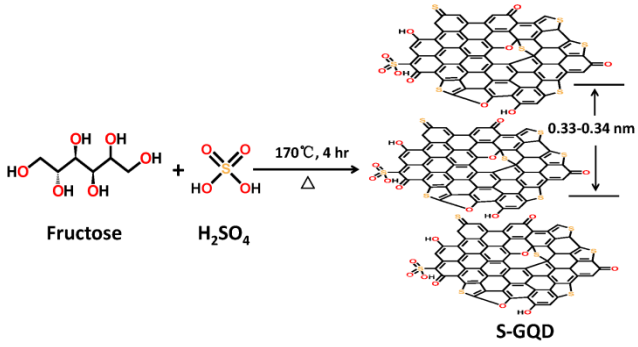

Scheme 1. The schematic illustration of the synthesis of the S-GQDs.

[a] *Solar Energy Research Institute, Yunnan Normal University, Kunming 650092, P. R. China. E-mail:pzhyang@hotmail.com*
[b] *Department of Applied Physics, The Hong Kong Polytechnic University, Hong Kong SAR, P. R. China. E-mail: apsplau@polyu.edu.hk*
[c] *Kunming Institute of Physics, Kunming 650223, P. R. China*

†Electronic supplementary information (ESI) available: The detailed information of chemicals, the FTIR, Raman, the STEM image and the C,O and S mapping of S-GQDs, the PLE spectra of S-GQDs, and the fitting parameters of PL decay curves of S-GQDs. See DOI: 10.1039/b000000x/

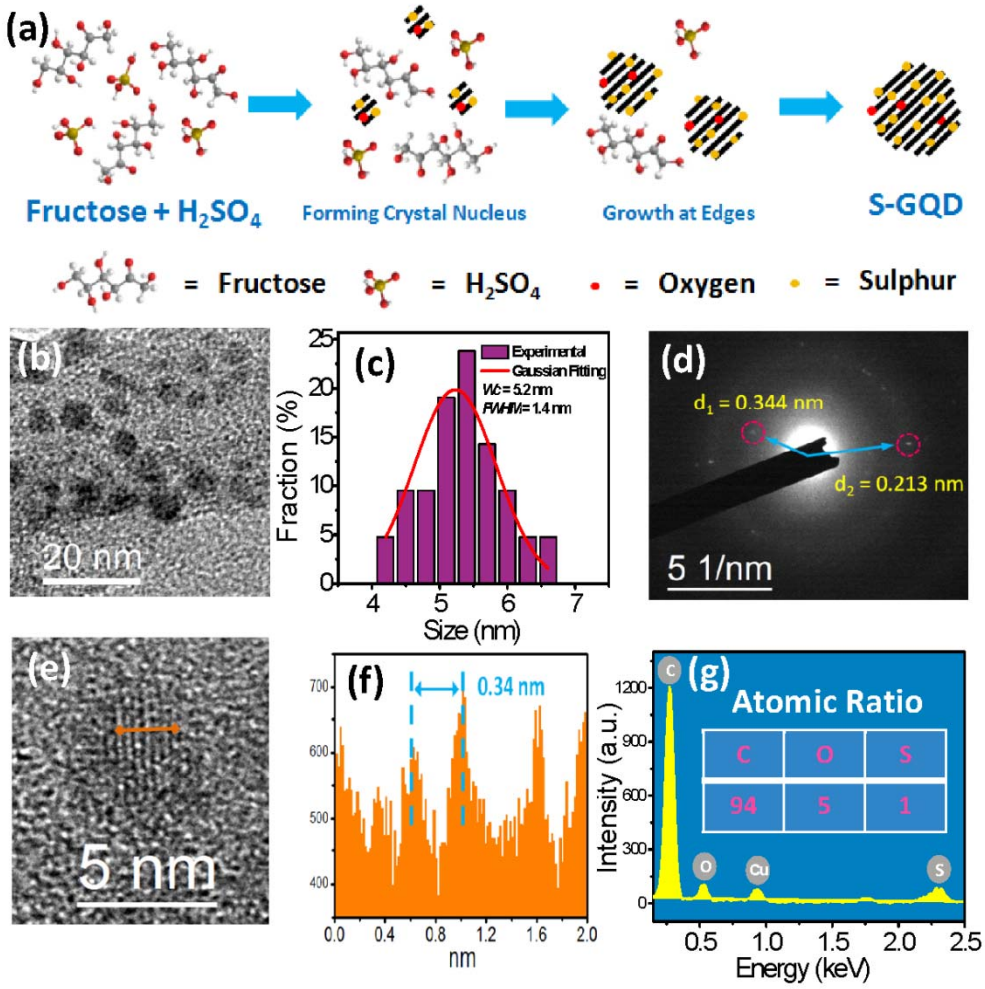

Fig. 1 (a) The growth process of the S-GQD. The black line represents a graphitic plane in the S-GQD. (b) The typical TEM image of the S-GQDs. (c) The size distribution of the S-GQDs. The red line is Gaussian fitting curve. The most frequent size is 5.2 nm with a FWHM value of 1.4 nm. (d) The electron diffraction pattern of the S-GQD indicates both in-plane (d_2 = 0.213 nm) and basal plane (d_1 = 0.344 nm) diffractions. (e) The HRTEM image of a single S-GQD, the lattice fringe is observed. (f) The line-profile analysis of the S-GQD as shown in (e). The *d* spacing is ~0.34 nm. (g) The EDS analysis on the S-GQDs, the atomic ratio of C/O/S is 94/5/1. The Cu peak comes from the TEM Cu grid.

morphology and height characterizations of the S-GQDs were performed by atomic force microscope (AFM) (Digital Instruments NanoScope IV) operating in the tapping mode. Raman scattering was measured using Horiba Jobin Yvon HR800 spectrometer using a laser with the wavelength of 488 nm. The Fourier transform infrared spectroscopy (FTIR) spectra of the samples were measured using the KBr pellet method by Nicolet 380 spectrometer with a resolution of 2 cm^{-1}. X-ray photoelectron spectroscopy (XPS) experiments were performed on a Kratos AXIS Ultra DLD X-ray photoelectron spectrometer with a monochromatic Al Kα X-ray source. X-ray diffraction (XRD) was carried out with a Rigaku SmartLab X-ray diffractometer (Cu K_α radiation λ =1.54056 Å) operating at 45 kV and 200 mA. The UV-Vis absorption spectra were recorded on a Shimadzu UV-2550 UV-Vis spectrophotometer. Photoluminescence (PL) measurements were performed using an FLS920P Edinburgh Analytical Instrument apparatus. For the excitation dependent emission spectra and photoluminescence excitation (PLE) spectra, Xe lamp was used as an excitation source. The time-resolved PL spectra of the S-GQDs were recorded using 375 nm picosecond pulsed laser (Model EPL375, Edinburgh Instruments) as an excitation source. The absolute quantum yield measurements were carried out using an integrating sphere (Edinburgh instruments, 150 mm in diameter coated with barium sulphate). The S-GQDs samples were placed in the cuvettes inside the integrating sphere. The S-GQDs samples were diluted with DI water to avoid reabsorption.

Results and discussions

Scheme 1 illustrates the growth process of the S-GQDs. Under hydrothermal condition (170℃, 4h), fructose molecules dehydrated inter- and intra- molecularly, forming honeycomb carbon matrix. Sulphuric acid catalyses the reaction and provides sulphur as a dopant. As shown in Figure 1a, the growth process of the S-GQDs involves in the following stages: Firstly, the crystal

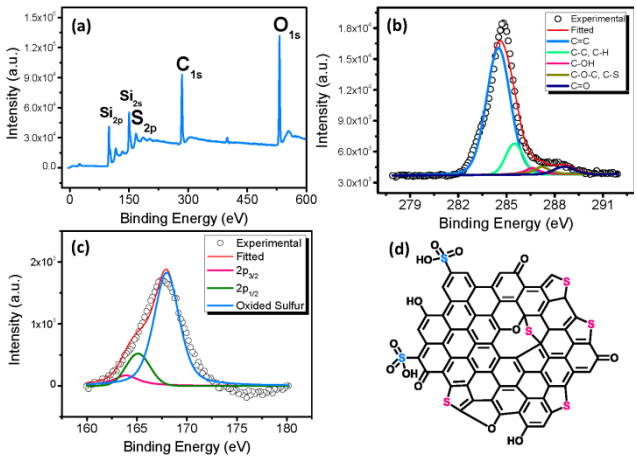

Fig. 2 (a) The full-scan XPS spectrum of the S-GQDs. The Si-related peaks come from the substrate. (b) The C1s XPS spectrum of the S-GQDs. (c) The S2p XPS spectrum of the S-GQDs. (d) The diagrammatically illustration of thiophene-S(pink) and oxide-S(blue) in the S-GQDs.

nucleus of S-GQDs are formed due to dehydration of fructose and sulphuric acid. Secondly, the growth of S-GQDs takes place at the surfaces (or edges) as chemically active functional groups are presented. Thirdly, the size of the S-GQDs grows with reaction time. Figure 1b shows the TEM image of the S-GQDs. The quantum dots show rounded shape with a relatively uniform size. The size distribution is found to obey a Gaussian distribution (Figure 1c), the most frequent size is 5.2 nm. The full-width-at-half-maximum (FWHM) value of the distribution curve is 1.4 nm, showing good monodispersed properties of our method.

The crystalline structure of the S-GQDs is revealed by the electron diffraction image as shown in Figure 1d. Two sets (d_1 = 0.344 nm and d_2 = 0.213 nm) of diffraction rings can be observed in Figure 1d, corresponding to basal plane spacing (d_1 = 0.344 nm) and in-plane lattice spacing (d_2 = 0.213 nm).[16-19] The HRTEM image is shown in Figure 1e. Figure 1f is the line-profile analysis of the S-GQD as shown in Figure 1e. Energy dispersive X-ray spectroscopy (EDS) analysis as shown in Figure 1g indicates that the atomic ratio of C/O/S is 94/5/1, showing the dominant element of the S-GQDs is C, sulphur is the minor doping element.

The doping of sulphur and its configuration were investigated by XPS. The full scan XPS spectrum of the S-GQDs is shown in Figure 2a. Three peaks located at ~167 eV,[10] ~284 eV [8] and ~532 eV [8] are S2p, C1s and O1s, respectively (O1s XPS signal is relatively high due to the contribution from the substrate SiO_2). The chemical bondings of C and sulphur are revealed by C1s (Figure 2b) and S2p (Figure 2c) spectra. As shown in Figure 2b, the C1s XPS spectrum can be deconvoluted into 5 small peaks, centred at 284.5 eV (C=C),[16] 285.5 eV (C-C, C-H) ,[16,18] 286.6 eV (C-OH),[20] 287.2 eV (C-O-C, C-S)[16,18] and 288.6 eV (C=O).[20] The C=C component is the most intense peak among all the deconvoluted peaks, meaning that C=C is the main C bonding

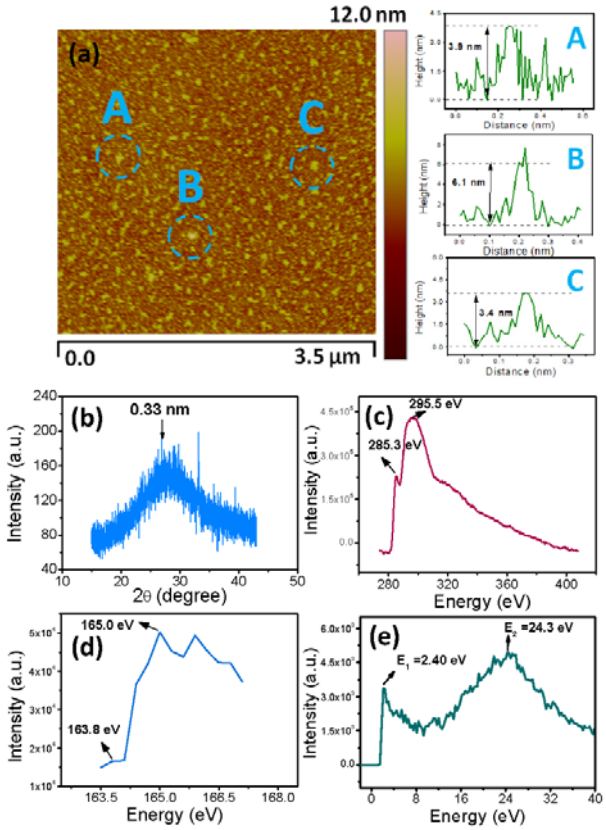

Fig. 3 (a) The AFM image of the S-GQDs assembled on Si substrate, dots A, B and C are randomly chosen S-GQDs, the corresponding height analyses have been shown on the right-hand side of AFM image. (b) The XRD pattern of the S-GQDs. (c) The EELS spectrum of C K-edge. (d) The EELS spectrum of S $L_{2,3}$-edge. (e) The low-loss EELS spectrum of the S-GQDs.

configuration which constructs the graphitic matrix structure. As for S 2p XPS spectrum, the peaks located at 163.9 eV and 165.1eV are $2p_{3/2}$ and $2p_{1/2}$ respectively of thiophene-S due to spin-orbit coupling.[7] The peak located at ~168.0 eV is the oxide-S.[7,13] Therefore the doped sulphur exists in two configurations, one is thiophene sulphur (pink, Fig.2d) and the other is oxide-sulphur (blue, Fig. 2d).

The FTIR spectra of the S-GQDs and the source are shown in Figure S1. The newly emerging peaks of the S-GQDs at ~455 cm^{-1} (C-S),[21] 1179 cm^{-1} (C=S) [2,15] and 1713cm^{-1} (C=S) indicate the effective doping of sulphur into carbon matrix. It should be noted that the presence of absorption peaks at ~1062 cm^{-1} (C-O) [12] and ~1635 cm^{-1} (C=O) [11,14] show that oxygen-containing functional groups are also contained in the S-GQDs as compared with the source fructose, both the two peaks of the S-GQDs are greatly reduced. The weakened absorptions at ~866 cm^{-1} (C-H)[16] and 2940 cm^{-1} (C-H) [16] suggest that the content of H is drastically decreased after the formation of S-GQDs.

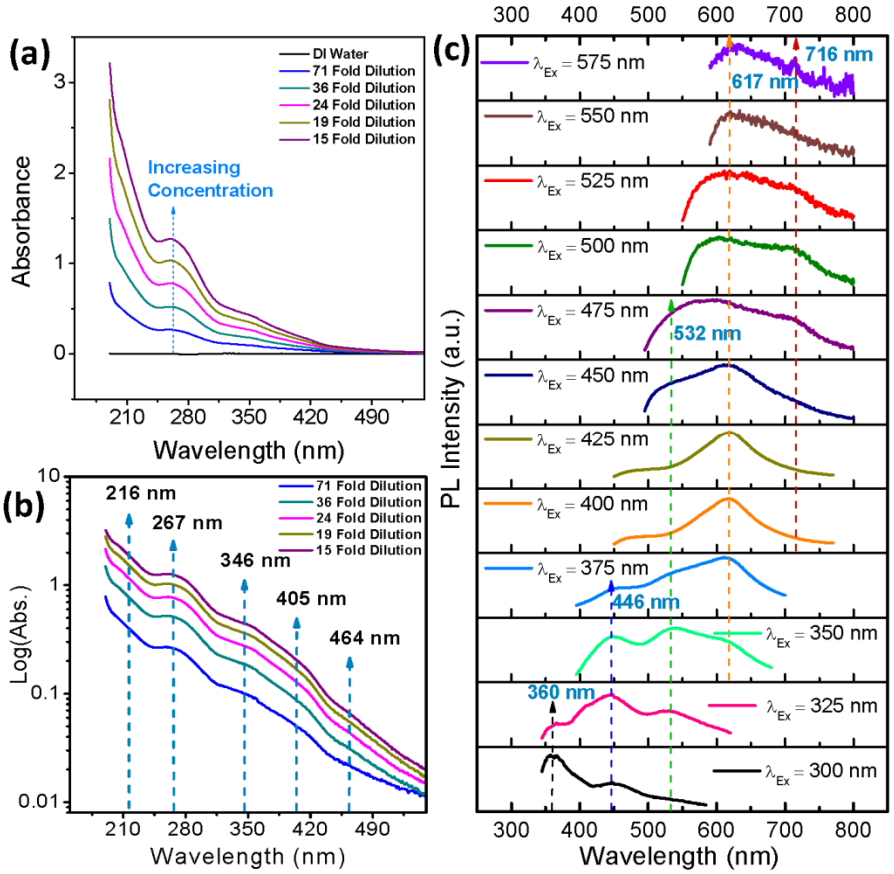

Fig. 4 (a) The UV-Vis absorption spectra of the S-GQDs at various concentrations. (b) The log(Absorbance) versus wavelength of the S-GQDs. (c) The PL spectra of the S-GQDs excited by various excitation wavelengths (λ_{Ex}).

The Raman spectra of the S-GQDs and the source fructose are shown in Figure S2. There are many dispersed small peaks superimposed on a very strong photoluminescence background which is peaked at ~2000 cm^{-1}, these small vibration peaks are as follows, 446.6 cm^{-1} (C-S), 583.3 cm^{-1} (C-H), 1088.6 cm^{-1} (C-OH),[17] 1272.0 cm^{-1} (C-O-C),[17] 1552.0 cm^{-1} (C=C, G peak, C=O), 2005.5 cm^{-1} (C=C=C),[19] 2385.9 cm^{-1}(C=C=O), 3004.5 cm^{-1} (C-H), 3328.2 cm^{-1} (O-H) and 3586.3 cm^{-1} (π *e* with O-H).[19] Combined with FTIR spectrum of the S-GQDs, the vibration spectra support the presence of sulphur in the S-GQDs.

The chemical composition is further demonstrated by elemental mappings, as shown in Figure S3. The scanning transmission electron microscopy (STEM) image of the S-GQDs (white dots) is shown in Figure S3a. Elemental carbon (blue), oxygen (red) and sulphur (green) mappings are performed on the samples, the content of C > O > S, which accords well with that of EDS results (Figure 1g).

Figure 3a is the AFM image of the S-GQDs assembled on Si substrate. The locations A, B and C are randomly chosen dots, their heights are 3.9 nm, 6.1nm and 3.4 nm respectively, yielding an average height of 4.5 nm, which is close to the size (5.2 nm) obtained from TEM. Figure 3b shows the XRD pattern of the S-GQDs. The diffraction curve is peaked at 2θ = 26.98° corresponding to a *d* spacing of 0.33 nm, which is similar to that of graphitic materials.[22,23]

Figure 3c shows the electron energy loss spectroscopy (EELS) of K-edge of C. The two energy peaks located at 285.3 and 295.5 eV correspond to $1s \rightarrow \pi^*$ and $1s \rightarrow \sigma^*$, respectively. The $L_{2,3}$-edge spectrum of S is shown in Figure 3d. There are two peaks located at 163.8 and 165.0 eV. For the low-loss EELS spectrum as shown in Figure 3e, the E_1 and E_2 are at 2.4 and 24.3 eV, respectively. It can be observed that E_1 (2.4 eV) of the S-GQDs is smaller than that of undoped GQDs (3.6 - 4.8 eV).[18] However, E_2 (24.3 eV) of the S-GQDs is higher than that of the undoped GQDs (22.8-24.0 eV),[18] probably due to the doping of S.

The UV-Vis absorption of the S-GQDs as a function of solution concentration is shown in Figure 4a. The log(Abs.) is plotted against wavelength as shown in Figure 4b, apparently, multiple absorption peaks located at 216, 267, 346, 405 and 464 nm are observed. It can also be observed that at a certain concentration, the absorbance of the S-GQDs increases with decreasing in wavelength. The larger the absorbance corresponds to larger intrinsic density of states (DOS) of the material.

Figure S4 shows the PLE spectra of the S-GQDs. It is noted that at the emission wavelength, λ_{Em}, larger than 460 nm, multiple peaks can be observed. The λ_{Em} influences both the shape and intensity of the PLE spectra. Multiple PLE peaks located at around 254, 308, 354, 373 and 415 nm, can be observed as the

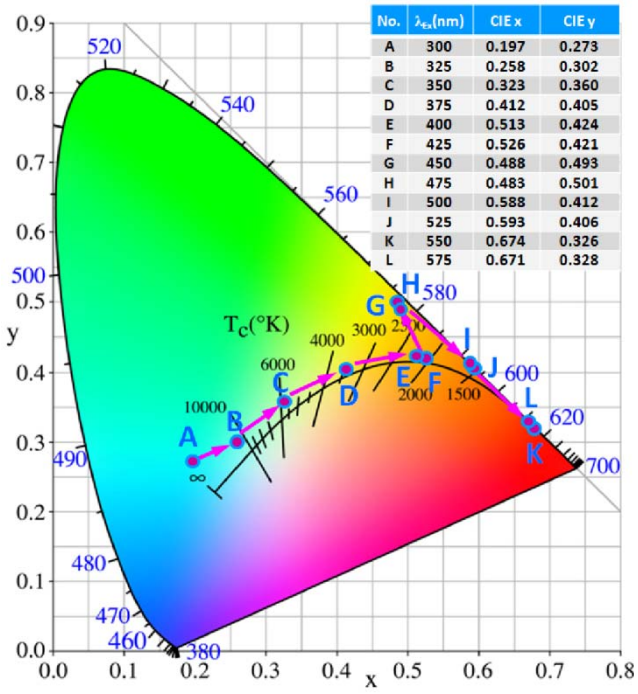

Fig. 5 The tunable optical emission of the S-GQDs as a function of λ_{Ex} as revealed by the chromaticity coordinates. The chromaticity coordinates are listed in the inset table. The emission colour covers blue, white, yellow, orange and red.

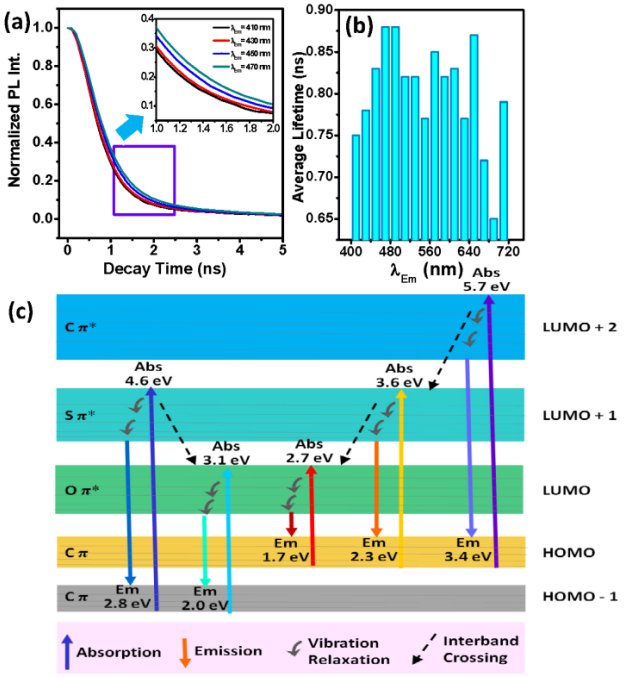

Fig. 6 (a) The time-resolved photoluminescence spectra recorded at different λ_{Em}. (b) The average lifetimes at different λ_{Em}. (c) The proposed energy level diagram of the S-GQDs.

λ_{Em} increases. The wavelengths of the PLE peaks correspond well to that of UV-Vis absorption peaks.

Figure 4c shows the PL spectra of the S-GQDs excited by various excitation wavelengths (λ_{Ex}). It can be apparently seen that the PL emissions (both shape and intensity) drastically depend on the λ_{Ex}. Multiple PL peaks at around 360, 446, 532, 617 and 716 nm can be observed when excited by various λ_{Ex}. The presence of multiple PL peaks is due to the existence of multiple electron transition pathways within the electronic structure of the S-GQDs. The doping of sulphur provides additional electron transition pathways for both absorption and PL emission, since the undoped GQDs only have two absorption peaks centered at 228 and 282 nm.[16,18]

The optical tunability of the S-GQDs can also be illustrated in Figure 5. As shown in Figure 5, the S-GQDs emit a variety of colours ranging from blue (A,B) (λ_{Ex} = 300, 325 nm), white (C) (λ_{Ex} = 350 nm), pale yellow (D) (λ_{Ex} = 375 nm), orange (E,F) (λ_{Ex} =400, 425 nm), greenyellow (G,H) (λ_{Ex} = 450, 475 nm), orange red (I,J) (λ_{Ex} =500, 525 nm), to red (K,L) (λ_{Ex} = 550, 575 nm). The corresponding chromaticity coordinates are listed in the inset of Figure 5.

Figure 6a shows the spectra of the time-resolved PL of the S-GQDs. It is found that PL decay can be affected by λ_{Em}. All the PL decay curves obey a triple-exponential model. In λ_{Em} range of 410 - 470nm, a shorter λ_{Em} may result in a fast decay. The average lifetime contains a fast component (τ_1: 0.48 - 0.65 ns) and two slow components (τ_2: 2.24 - 3.09 ns; τ_3: 18.5 2- 120 ns). The slow components are regarded as correlating with minor element components S and O.[16] Compared with chlorine doped GQDs (<τ>: 0.77-1.09 ns) [19] with a similar size (~ 5 nm), the S-GQDs exhibit a shorter average lifetime (<τ>: 0.65 - 0.88 ns) as shown in Figure 6b and Table S1. The difference in lifetime is probably due to a more effective electron transition in the S-GQDs. The PL quantum yield (QY) of the S-GQDs was measured to be 7.1% by the absolute QY measurement method using a λ_{Ex} of 375nm. The value is comparable to the undoped GQDs.[16,18]

Based on the above results, the energy level diagram of the S-GQDs is deduced as shown in Figure 6c. The presence of sulphur introduces additional energy levels between π and π^* of carbon. It should be noted that the excited electron may emit longer wavelengths through interband crossing, as revealed by PLE spectra (Figure S4). More PLE peaks are presented at longer λ_{Em} because of the interband crossing of electrons from higher energy levels.

The absorption of photons with energies of 5.7 eV (216 nm), 4.6 eV (267 nm), 3.6 eV (346 nm), 3.1 eV (405 nm) and 2.7 eV (464 nm) induces multiple pathways of electron transitions in the S-GQDs. The photons stay at the excited state for 0.65 - 0.88 ns (average lifetime). The radiative recombination will then take place after vibration relaxation and interband crossing, emitting photons with energy of 3.4 eV (360 nm), 2.8 eV (446 nm), 2.3 eV (532 nm), 2.0 eV (617 nm) and 1.7 eV (716 nm). The emitted photon has smaller energy compared to the absorbed photon because of the Stokes shift. The introduction of sulphur increases the pathways of electron transition both in absorption and PL emission, thus, the presence of sulphur-related energy level plays an important role in tuning the electronic structure and optical properties of the S-GQDs.

Conclusions

We fabricated monodispersed crystalline S-GQDs. The doped sulphur exists in the two configurations, *i.e.* thiophene-S and oxide-S. Sulphur doping can modulate the electronic structure of the S-GQDs. The effective doping (1% atomic) of sulphur introduces S-related energy levels between π and π^* of C. The additional energy levels diversify the electron transition pathways. The S-GQDs can emit a variety of colours ranging from blue to white, pale yellow, orange, greenyellow, orange red and red, covering most of colours in the visible light. The study indicates that sulphur doping effectively tunes the optical properties of GQDs, showing great potential applications in optoelectronics and photonics for their simple, scalable, and low-cost preparation.

Acknowledgements

This work was financially supported by the National Natural Science Foundation of China (Grant No.61106098, 61066004 and U1037604), the Research Grants Council of Hong Kong (Project No. PolyU 5006/12P), HK PolyU grants (Project Nos. G-YJ70 and 1-ZV8N), and the Key Project of Applied Basic Research of Yunnan Province (Project No. 2012FA003).

Notes and references

1 Z. Yang, Z. Yao, G. Li, G. Fang, H. Nie, Z. Liu, X. Zhou, X. Chen and S. Huang, *ACS Nano*, 2012, **6**, 205-211.
2 Y. Xia, Y. Zhu and Y. Tang, *Carbon*, 2012, **50**, 5543-5553.
3 M. Seredych, K. Singh and T. J. Bandosz, *Electroanalysis*, 2013, **25**, P.
4 Y. Li, J. Wang, X. Li, D. Geng, M. N. Banis, Y. Tang, D. Wang, R. Li, T.-K. Sham and X. Sun, *J. Mater. Chem.*, 2012, **22**, 20170-20174.
5 T. J. Bandosz, J. Matos, M. Seredych, M. S. Z. Islam and R. Alfano, *Appl. Catal. A: Gen*, 2012, **445-446**, 159-165.
6 H. Gao, Z. Liu, L. Song, W. Guo, W. Gao, L. Ci, A. Rao, W. Quan, R. Vajtai and P. M. Ajayan, *Nanotechnology*, 2012, **23**, 275605.
7 S. Yang, L. Zhi, K. Tang, X. Feng, J. Maier and K. Müllen, *Adv. Funct. Mater.*, 2012, **22**, 3634-3640.
8 I.-Y. Jeon, S. Zhang, L. Zhang, H.-J. Choi, J.-M. Seo, Z. Xia, L. Dai and J.-B. Baek, *Adv. Mater.*, 2013, **25**, 6138-6145.
9 J. Liang, Y. Jiao, M. Jaroniec and S. Z. Qiao, *Angew. Chem. Int. Ed.*, 2012, **51**, 11496-11500.
10 S.-A. Wohlgemuth, R. J. White, M.-G. Willinger, M.-M. Titirici and M. Antonietti, *Green Chem.*, 2012, **14**, 1515-1523.
11 M. Zheng, H. Zhang, Y. Xiao, H. Dong, Y. Liu, R. Xu, Y. Hu, B. Deng, B. Lei and X. Liu, *Mater. Lett.*, 2013, **109**, 279-282.
12 M. Seredych and T. J. Bandosz, *Fuel*, 2013, **108**, 846-849.
13 Y. Yan, Y.-X. Yin, S. Xin, Y.-G. Guo and L.-J. Wan, *Chem. Commun.*, 2012, **48**, 10663-10665.
14 D. Sun, R. Ban, P.-H. Zhang, G.-H. Wu, J.-R. Zhang and J.-J. Zhu, *Carbon*, 2013, **64**, 424-434.
15 D. Qu, M. Zheng, P. Du, Y. Zhou, L. Zhang, D. Li, H. Tan, Z. Zhao, Z. Xie and Z. Sun, *Nanoscale*, 2013, **5**, 12272-12277.
16 L. Tang, R. Ji, X. Cao, J. Lin, H. Jiang, X. Li, K. S. Teng, C. M. Luk, S. Zeng, J. Hao and S. P. Lau, *ACS Nano*, 2012, **6**, 5102-5110.
17 L. Tang, R. Ji, X. Li, K. S. Teng and S. P. Lau, *J. Mater. Chem. C*, 2013, 1, 4908-4915.
18 L. Tang, R. Ji, X. Li, K. S. Teng and S. P. Lau, *Part. Part. Syst. Charact.*, 2013, **30**, 523-531.
19 X. Li, S. P. Lau, L. Tang, R. Ji and P. Yang, *J. Mater. Chem. C*, 2013, **1**, 7308-7313.
20 L. Tang, X. Li, R. Ji, K. S. Teng, G. Tai, J. Ye, C. Wei and S. P. Lau, *J. Mater. Chem.*, 2012, **22**, 5676-5683.
21 K. Y. Chernichenko, V. V. Sumerin, R. V. Shpanchenko, E. S. Balenkova and V. G. Nenajdenko, *Angew. Chem. Int. Ed.*, 2006, **45**, 7367-7370.
22 C. Oshima and A. Nagashima, *J. Phys.: Condens. Matter.*, 1997, **9**, 1-20.
23 L. B. Biedermann, M. L. Bolen, M. A. Capano, D. Zemlyanov and R. G. Reifenberger, *Phys. Rew. B.*, 2009, **79**, 125411.

TOC

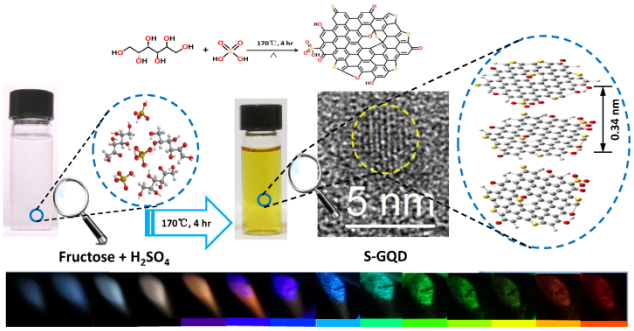

We demonstrate sulphur doping which can effectively tune the electronic structure and optical properties of S-GQDs by introducing S-related energy levels within the electronic structure.